Received: 6 July 2023 | Accepted: 22 August 2023

DOI: 10.1002/agg2.20422

Agrosystems, Geosciences & Environment OPEN ACCESS

ORIGINAL ARTICLE

Agrosystems

Automatic zone management definition in Mediterranean environment for *Triticum durum*

Roberto Orsini | **Marco Fiorentini** | **Stefano Zenobi** | **Rodolfo Santilocchi** | **Paola A. Deligios** | **Luigi Ledda**

Dipartimento di scienze agrarie, ambientali e alimentari, UniversitÃ Politecnica delle Marche, Ancona, Italy

Correspondence
Marco Fiorentini, Dipartimento di scienze agrarie, ambientali e alimentari, UniversitÃ Politecnica delle Marche, Ancona, Marche, Italy. Email: m.fiorentini@univpm.it

Assigned to Associate Editor Calogero Schillaci.

Funding information
University Strategic Project, Grant/Award Number: PSA 2017; Horizon Project 2020 SolaQua, Grant/Award Number: 952879; PSR Marche 2014/2020 Precision agriculture: reduction of the environmental impact of production systems, Grant/Award Number: ID.29000

Abstract

Precision agriculture (PA) is an agronomic management that allows the parsimonious use of agronomic inputs according to the crop's actual spatiotemporal needs. The most important agronomic practice of PA is the site-specific management (SSM) of agronomic inputs. To apply SSM, the number and location of homogeneous zones must be defined. Nowadays, many approaches are used to define the number of zones in an arbitrary and constant way, such as high-, medium-, and low-input zones, without a priori statistical analysis. Two combined field experiments were carried out on durum wheat (*Triticum turgidum* subsp. *durum* Desf.) in central Italy to agronomically validate an automatic approach aimed at defining the number and position of the homogeneous zones using multispectral images. For both sites, at stem elongation and anthesis, the dry biomass per square meter and Soil Plant Analysis Development (SPAD) readings were measured, while at crop maturity the yield was measured. This approach uses multispectral images as source data and uses the gap statistic index to determine the correct number of zones. The management zones created were well-fitted with the experimental design of both sites, and the validation was made by the statistical analysis performed on yield data, SPAD, dry biomass, and normalized difference red edge index with an average difference of 40.2%, 28.5%, 57.5%, and 37.4%, respectively, between the management zones. The approach could be scaled by using the multitemporal multispectral images provided by satellite constellation, which enables farms and societies to take advantage of all the economic and environmental benefits of PA.

1 | INTRODUCTION

The agriculture sector is the major source of diffusion and pollution of nitrogen (N), which impacts several issues such as economic, environmental, and social ones (Puertes et al., 2021). When nitrogen use efficiency is not high, groundwater quality (Rath et al., 2021), air pollution (Peng et al., 2020), and net farm profit are negatively affected

Abbreviations: ANOVA, analysis of variance; C/N, carbon-nitrogen ratio; CT, conventional tillage; LTE, long-term experiment; NDRE, normalized difference red edge index; PA, precision agriculture; SPAD, Soil Plant Analysis Development; SSM, site-specific management; UAV, unmanned aerial vehicle.

This is an open access article under the terms of the Creative Commons Attribution License, which permits use, distribution and reproduction in any medium, provided the original work is properly cited.
© 2023 The Authors. *Agrosystems, Geosciences & Environment* published by Wiley Periodicals LLC on behalf of Crop Science Society of America and American Society of Agronomy.

(Langholtz et al., 2021). Moreover, the technology that allows N fixation leads to the generation of mineral fertilizers and requires large amounts of energy, mostly provided by fossil fuel energy (Chai et al., 2019).

The European Commission is requesting an effort from the agronomic scientific community to perform a transition from traditional farming systems to more sustainable ones (Wesseler, 2022) to accomplish the "Farm to Fork" strategy, which constitutes one of the critical components of the European Green Deal (https://ec.europa.eu/info/sites/info/files/europe-an-green-deal-communication_en.pdf) and Farm to Fork Strategy (https://ec.europa.eu/food/farm2fork_en-15/01/2021).

The Farm to Fork strategy aims to reduce nutrient losses by at least 50%, while ensuring no deterioration in soil fertility. At the same time, a reduction in fertilizer use by at least 20% is expected by 2030. To achieve this ambitious goal, the scientific community is focusing on the development of innovative cropping systems (Deligios et al., 2019), spread of conservative agriculture (Capmourteres et al., 2018), application of the principles of organic farming (Migliorini et al., 2014), and precision agriculture (PA; Argento et al., 2020).

Although N fertilization has several negative environmental and social impacts, it improves crop yield and income. Without N input, it is estimated that only about half of the current global population can be supplied with sufficient food, energy, and protein (Dawson & Hilton, 2011).

In the Mediterranean, winter cereals are the dominant crops (Tsialtas et al., 2018), and the most important key driver for achieving maximum productivity in durum wheat is the N fertilization if water is not a limiting factor (Orsini et al., 2019a).

An opportunity exists to further enhance the yield, profitability, and nutrient use efficiency of these systems through site-specific management (SSM), which is the most common practice of PA applications. The PA technologies and applications can lead to higher N use efficiency, therefore reducing the environmental impact of agriculture activities and the overall cost of production (Capmourteres et al., 2018).

In order to apply SSM, it is necessary to perform a continuous monitoring activity of the crop status during the growing seasons with spatial-temporal data, which can be performed by using (1) a network of proximal sensors (Aqeel-Ur-Rehman et al., 2014), or alternatively (2) remote-sensing technologies (Maes & Steppe, 2019), or through a (3) combination of remote and proximal sensors (Munnaf et al., 2021).

Greater attention is currently being devoted to data fusion techniques (Pantazi et al., 2020) that have the capability to fuse data with different spatial–temporal resolutions for delineating zone management for PA applications. Castrignanò et al. (2018) propose a multivariate geostatistical sensor data fusion approach to combine ground penetrating radar and electromagnetic induction sensor for delineating homogeneous zones in terraced olive groves under organic cropping. Other data fusion techniques are developed using machine learning (Fiorentini et al., 2022) and deep learning (Schillaci et al., 2021) methods to handle different types of inputs and nonlinear tasks (Chlingaryan et al., 2018).

Based on the type of spatial–temporal data, we can perform different workflow analyses to delineate management zone (Nawar et al., 2017). Whelan and Mcbratney (2003) suggested five steps to create and verify zones based on (1) creation of data layers, (2) interpolation of data layers, (3) cluster analysis, (4) determining the confidence of interval, and (5) guided soil sampling to assess the soil-related causes of between-zone variability. Albarenque et al. (2016) suggested an approach based on the use of a crop deterministic model to determine the spatial–temporal variability of soil–crop–climate data and then define the homogeneous zones.

However, to apply SSM, it is important to define the number and location of homogeneous zones, which have a great impact on the agronomic input efficiency, the potential yield per unit area, and the environment-economic benefit of the PA (Denora, Fiorentini, et al., 2022). Nowadays, there are several approaches to define the number and location of homogeneous zones a priori using operational software, without performing an analysis. Several authors reported the presence of three different homogeneous zones (e.g., high, medium, and low) without specifying the approach or calculation that led to the creation of that number of homogeneous zones, and these arbitrary choices impact negatively the environmental and economic benefit of the PA.

As SSM is an operational practice, all methods must be designed and validated for use at an operational scale. For a method to be considered operational, it must meet the following five criteria: (1) it must be automatic, (2) scalable, (3) its data source must be free and temporally-spatially accurate (e.g., multispectral satellite data), (4) it must be applicable to use in any field, (5) it must be easy to use, and (6) scientifically validated (Zhang et al., 2010).

Core Ideas

- Multi-site/year field experiments were carried out on durum wheat in central Italy.
- Agronomic validation of automatic zone management delineation approach was set up.
- The management zone well-fitted with the experimental sites.
- The approach could be scaled up by using satellite multispectral data.

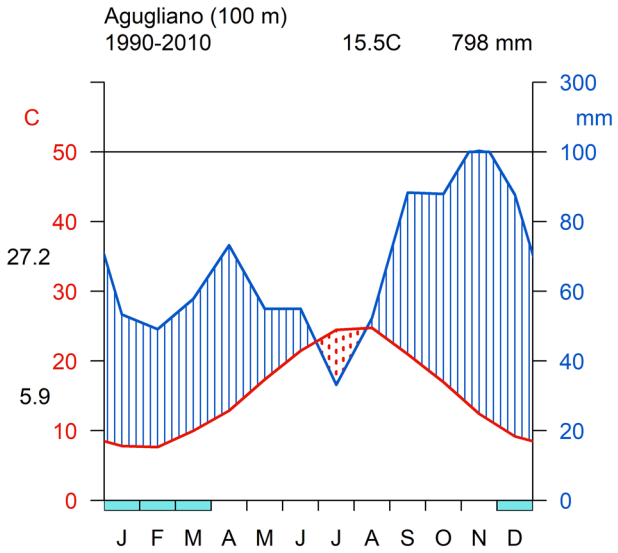


FIGURE 1 Walter and Lieth climate diagram of Agugliano weather station (1990–2010 long-term series provided by the Agenzia Servizi al Settore Agroalimentare delle Marche [ASSAM]).

Several authors explored different source data to define zone management, such as yield mapping data (Gavioli et al., 2019; Stettmer et al., 2022), electromagnetic sensors (Denora, Amato, et al., 2022; Yuan et al., 2022), and grid-georeferenced soil samples (Ali et al., 2022; Vallentin et al., 2020), but such data sources are difficult to put into operational because they are expensive, time-consuming, have a low temporal resolution, and use proximal sensors.

In this manuscript, an advancement in knowledge has been proposed by agronomically validating an automatic workflow analysis that can define the number and location of the zone management with multi-site/year yield data and different experimental designs. Once validated, this approach could be scaled up by using the source data of the multispectral images acquired by the private and public satellite constellations to automate the generation of prescription maps for rainfed Mediterranean durum wheat and thus facilitate the adoption of these agronomic techniques, enabling farms and society to take advantage of all the economic and environmental benefits of PA.

2 | MATERIALS AND METHODS

2.1 | Long-term experiment description

The long-term experiment (LTE) is located at the "Pasquale Rosati" experimental farm of the Polytechnic University of Marche in Agugliano, Italy (43°32′ N, 13°22′ E, 100 a.s.l.). According to the Walter and Leith climatic classes, the climate of the study area (Figure 1) is attenuated meso-Mediterranean, and it is characterized by a mean annual precipitation of approximately 798 mm and a mean annual temperature of 15.5°C with monthly means ranging from 7.4°C in February to 24.1°C in August.

During the 2017–2018 crop growing season, the highest cumulative precipitation (647 mm) was recorded, while the 2018–2019 and 2019–2020 growing seasons recorded a contraction of 36% (414 mm) and 22% (506 mm), respectively. The mean yearly temperature in the 2019–2020 growing season was 1°C higher than the previous growing seasons (Table 1).

The soil of the study area is classified as Calcaric Gleyic Cambisols with a silt-clay texture, 9.1 g kg^{-1} of organic carbon, 13.8 mg kg^{-1} of extractable phosphorus, 323.2 mg kg^{-1} of exchangeable potassium, 26.7 mEq 100 g^{-1} of cation exchange capacity, pH of 8.1, 29.6% of field water capacity of the weight, 17.6% of wilting point, and a slope of approximately 10%.

2.1.1 | LTE design and management practices

The LTE, established in 1994 and still in use (Seddaiu et al., 2016), consists of a rainfed 2-year rotation of durum wheat (*Triticum turgidum* L. subsp. *durum* Desf.) cv. Tyrex (Apsov Sementi) and maize (*Zea mays* L.) cv. DK440 (hybrid, FAO Class 300, Dekalb—Monsanto Agricoltura Italia S.p.A). The crop rotation was duplicated in two adjacent fields to allow for all crops to be present each year (Figure 2).

Within each field, three soil management (main plot, 1500 m^2 each) systems (conventional, reduced tillage, and no tillage) and three N fertilizer (subplot, 500 m^2 each) levels were arranged according to a split-plot experimental designs with two randomized blocks and repeated in the same plots every year.

The conventional tillage (CT), which is representative of the business-as-usual tillage practice in the study area, and the reduced tillage plots were plowed along the maximum slope every year by a mouldboard (with two plows) at a depth of 40 cm or a chisel at a depth of 25 cm in autumn for wheat and in summer for maize, respectively. The seedbed was prepared by harrowing before the sowing date. The three N fertilizer treatments were N0, N90, and N180, corresponding to 0, 90, and 180 kg N ha^{-1} distributed in two rates for wheat and maize.

In this manuscript, the research activity focused on durum wheat plots where CT and the three N levels were applied for 3 years (2018–2020) in growing seasons. The CT plots were chosen because it was comparable with the soil management conducted at the "Guzzini" farm.

The N90 treatment was compliant with the agri-environmental measures adopted within the rural development plans at a local scale. The N180 treatment was the business-as-usual N rates in the study area at the start of the experiment.

TABLE 1 Thermo-pluviometric trend during the study period (2017–2020) and the long-term period (1990–2010) recorded by the Agugliano station.

Months	November	December	January	February	March	April	May	June	July
Cumulative rainfall (mm)									
2017–2018	24	96	29	173	143	37	95	48	2
2018–2019	0	61	70	22	36	59	165	1	0
2019–2020	0	0	4	17	158	119	142	61	5
Long-term data	104	88	53	49	58	73	55	55	33
Mean temperature (°C)									
2017–2018	10	7	9	5	9	16	19	23	26
2018–2019	5	7	5	8	12	13	15	25	28
2019–2020	13	6	7	11	10	14	19	22	25
Long-term data	12.1	8.9	7.5	7.4	9.7	12.6	17.2	21.4	24.5

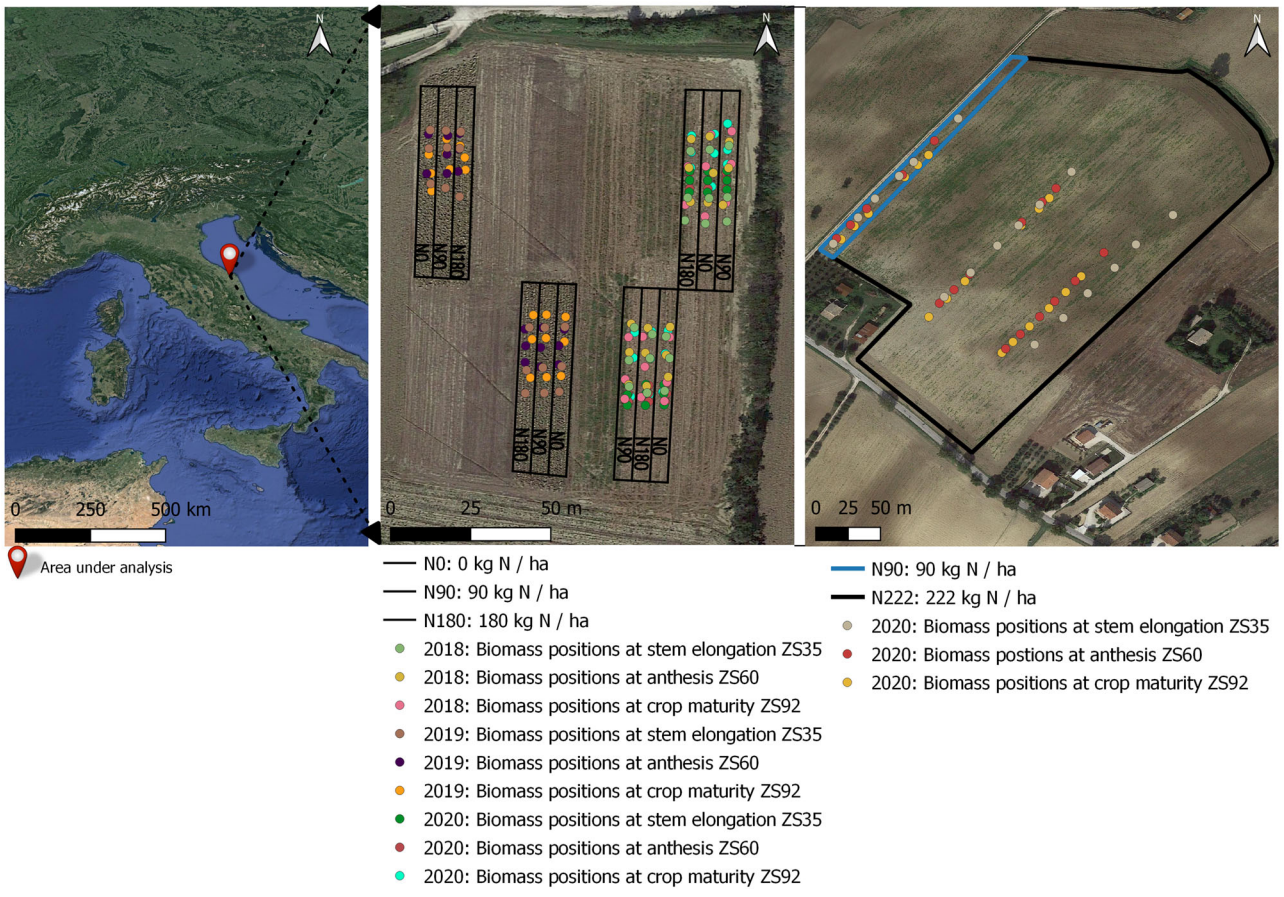


FIGURE 2 Long-term experiment (LTE) site (center) and farm site (right), planimetry, and georeferenced positions of sampling biomass points.

Durum wheat was sown at the beginning of autumn at a seeding rate of 220 kg ha^{-1} with a between-row distance of 0.17 m. Each year, N fertilization in the form of urea (46%) was split into two applications: 50% at the end of tillering and 50% before head emergence. Weeds, pests, and diseases were chemically controlled. The sequence of agronomic practices applied at the LTE is reported in Table 2.

2.2 | Farm-scale experiment description

Farm-scale experiment (Farm) was carried out during the 2019–2020 growing season in the "Francesco Guzzini" farm located in Recanati (43° 23′ N, 13° 31′ E, 115 a.s.l.), central Italy (Figure 2). The climate is attenuated meso-Mediterranean. The mean annual precipitation is 711 mm

TABLE 2 Agronomic management practices adopted during the 3-year experimental period (mm/dd/yyyy).

Agro-technique	2018	2019	2020
Ploughing	10/02/2017	09/26/2018	11/11/2019
Harrowing and seedbed preparation	11/20/2017	11/01/2018	11/25/2019
Sowing	11/21/2017	11/30/2018	12/27/2019
Weed control: Pinoxaden[a]	03/28/2018	03/08/2019	02/10/2020
N fertilization	03/29/2018	03/18/2019	02/25/2020
	04/30/2018	05/02/2019	04/09/2020
Pest control: Azoxystrobin, cyproconazole[b]	04/24/2018	04/22/2019	04/20/2020
Harvest	07/06/2018	07/07/2019	07/06/2020

[a]Dose: 30 g ha^{-1} of active ingredient.
[b]Dose: 0.16 L ha^{-1} of active ingredient.

TABLE 3 Thermo-pluviometric trend during the study period (2019–2020) and the long-term period (1990–2010) recorded by the Recanati station.

Months	November	December	January	February	March	April	May	June
Cumulative rainfall (mm)								
2019–2020	13	64	30	26	128	44	44	50
Long-term data	96	84	50	48	51	65	51	47
Mean temperature (°C)								
2019–2020	12.6	9.0	6.5	10.1	10.1	13.5	18.5	21.8
Long-term data	12.3	9.2	7.9	7.7	10.0	12.8	17.4	21.7

and the mean annual temperature is 15.9°C with monthly means ranging from 7.7°C in February to 24.7°C in August. During the 2019–2020 crop growing season, the farm site was characterized by a seasonal rainfall close to 400 mm (about 100 mm lower than the precipitation recorded at the Agugliano weather station during the same growing season) and mean temperatures of 1.5°C lower than temperature recorded at Agugliano (Table 3).

The soil of the farm site is classified as Calcaric Gleyic Cambisols with a silt-clay texture, with 8.4 g kg^{-1} of organic carbon, 10.3 mg kg^{-1} of extractable phosphorus, 283.2 mg kg^{-1} of exchangeable potassium, 28.0 mEq 100 g^{-1} of cation exchange capacity, 8.1 of pH, 28.5% of field water capacity of the weight, 16.2% of wilting point, and a slope of about 6%.

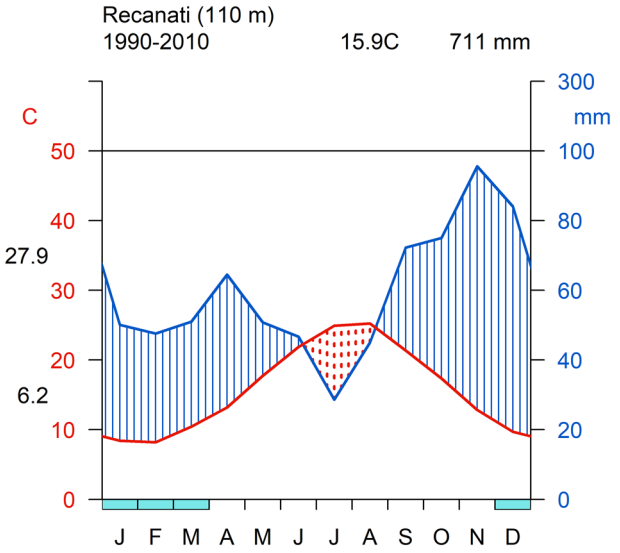


FIGURE 3 Walter and Lieth climate diagram of Recanati weather station. Period of observation: 1990–2010.

2.2.1 | Farm-scale experiment design and management practices

The farm site was chosen because it had the same agronomic management (Figure 3) as that of the LTE site. Indeed, the farm site has a rainfed 2-year crop rotation with durum wheat and maize. In both cases, the same cultivars were adopted in the LTE experiment in detail cv. Tyrex and cv. DK440 (hybrid, FAO Class 300, Dekalb—Monsanto Agricoltura Italia S.p.A).

The soil is managed with CT, where two N levels were applied in two adjacent areas (Figure 2). The preparation of the seedbed was performed as reported in the LTE site, with plowing performed along the maximum slope by a mouldboard plow (with two plows) at a depth of 0.4 m in autumn. Before seeding, a harrowing operation has been performed

TABLE 4 Agronomic management practices adopted in the farm site during the experimental period (mm/dd/yyyy).

Agro-technique	2020
Ploughing	10/02/2019
Harrowing and seedbed preparation	11/11/2019
Sowing	11/15/2019
Weed control: Pinoxaden[a]	04/22/2020
N fertilization	01/20/2020
	03/20/2020
Pest control: Azoxystrobin, cyproconazole[b]	04/22/2020
Harvest	06/28/2020

[a]Dose: 25 g ha^{-1} of active ingredient.
[b]Dose: 0.13 L ha^{-1} of active ingredient.

while the sowing has been done with a seed rate of 220 kg ha^{-1} with a row spacing of 0.17 m.

The two N levels correspond to 90 and 222 kg N ha^{-1} and were distributed at two rates. Each rate contains half of the total N and was applied to the crop in the form of urea (46% N) at the end of tillering and the last rate is applied before head emergence. Weeds, pests, and diseases were chemically controlled. The sequence of agronomic practices applied at the farm site is reported in Table 4.

2.3 | Measurements

To characterize the soil properties, a soil sampling campaign was carried out in 2019 for both sites, with a hand auger (model: Suelo HA-3, Zhejiang Lujian Instrument Equipment Co., Ltd.) immediately before sowing. From each plot of the LTE site, three samples were taken at a depth of 0–0.3 m and georeferenced using the Leica Zeno 20 (Leica Geosystem). While for the farm site for both N areas, four samples were taken using the same procedure reported for the LTE site.

Using the soil organic matter with the Walkley–Black chromic acid wet oxidation method and the total N availability with the Kjeldahl method, it has been analyzed that the ratio of carbon-nitrogen (C/N) is the same as the ratio of previous measures.

For each field survey day, Soil Plant Analysis Development (SPAD) readings (Konica Minolta Sensing 2003, Osaka, Japan) and the dry biomass per square meter (g m^{-2}) at stem elongation and anthesis phenological stages (ZS35 and ZS60 respectively where ZS = Zadoks Scale) were recorded (Zadoks et al., 1974).

For each plot of the LTE site, three test areas were randomly selected and georeferenced by using the Leica Zeno 20 (Leica Geosystem). At each test area, 10 leaves were chosen to make the SPAD readings. The readings were taken on the central and distal portion of the leaves, at the same tune slot, around midday (11:00 a.m.–13:00 p.m.). For the farm site, test areas were randomly selected in the N90 and N222 areas (Figure 2) and on which the SPAD readings were performed. After performing the SPAD readings, at each test area, fresh plant biomass was manually cut and collected in a 0.5 m long row. The fresh plant biomass was oven-dried at 80°C for 48 h and weighed (g). Starting from the dry biomass weight (g), we calculated the dry biomass per square meter (g m^{-2}) by using the equation:

$$\text{Dry biomass } \left(\text{g m}^{-2}\right) = \frac{\text{Dry biomass (g)}}{a \times b}$$

where a is the length of the sampling area, and b is the row spacing. Before each sampling activity, multispectral images were acquired (MAIA S-2, SAL engineering) by using an unmanned aerial vehicle (UAV) platform (DJI Matrice 600 pro, SZ DJI Technology Co., Ltd.) to compute the normalized difference red edge index (NDRE) (Barnes et al., 2000). At crop maturity (ZS92), the grain yield (t ha^{-1}) has been measured by using a laboratory thresher for three test areas (1 m long row) per plot.

2.3.1 | Remote sensing application

Multispectral images were acquired at stem elongation (ZS35) and anthesis (ZS60) phenological stages for each growing season under analysis. To avoid the variation in sun radiation during the flight, the UAV was equipped with an incident light sensor that can record the light variation and then correct the nine spectral bands of the MAIA S-2. Moreover, six ground control points have been positioned for the image post-processing to improve the spatial accuracy of the image. All the relevant flight settings are given in Table 5.

Each image acquired by a UAV flight requires an image processing operation to reduce noise, convert to the right file format, and prepare all image datasets for the orthomosaic map generation process. The image processing is composed of four main steps: (1) convert raw image file format to tiff image file format, (2) orthomosaic reflectance map generation, (3) computation of vegetation index map, and (4) data extraction.

The raw multispectral images were exported from the multispectral cameras to the computer. The dedicated software MultiCam Stitcher Pro (SAL engineering & Eoptis) was used to convert the raw format image to the multichannel tiff format. In this process, the light variation correction to the images was also performed, thanks to the incident light sensor equipped on the UAV platform.

To generate the orthomosaic reflectance maps, the Agisoft Metashape (Agisoft LLC) was used. The software is based on a structure from a motion algorithm (Verhoeven, 2011).

TABLE 5 Flight setting information.

Site	Phenological stage	Date (mm/dd/yyyy)	Sensor	F-S overlap (%)	MOF
LTE	ZS35	04/28/2018	MAIA S-2	75–65	Automatic
	ZS60	05/27/2018	MAIA S-2	75–65	Automatic
LTE	ZS35	04/18/2019	MAIA S-2	75–65	Automatic
	ZS60	05/24/2019	MAIA S-2	75–65	Automatic
LTE	ZS35	02/23/2020	MAIA S-2	75–65	Automatic
	ZS60	04/02/2020	MAIA S-2	75–65	Automatic
Farm site	ZS35	03/19/2020	MAIA S-2	75–65	Automatic
	ZS60	04/24/2020	MAIA S-2	75–65	Automatic

Abbreviations: F-S, forward-side overlap; LTE, long-term experiment; MOF, mode of flight; ZS, Zadoks scale; ZS35, stem elongation; ZS60, anthesis.

To complete the third and fourth main steps, the orthomosaic reflectance map was imported into R statistical software (ver. 3.5.1., 2018), and then the "stack" function of the raster R package (Hijmans et al., 2011) was used. Based on the previous studies (Orsini et al., 2019b), the NDRE (Barnes et al., 2000) vegetation index had a higher correlation accuracy with the durum wheat crop parameters than the other vegetation indexes, so the NDRE was computed by using the following formula:

$$\text{NDRE} = \frac{\text{NIR} - \text{Red Edge}}{\text{NIR} + \text{Red Edge}}$$

where NIR is the near-infrared spectral band (865 nm) and Red Edge is the red edge spectral band (705 nm). To extract the NDRE values only at the points where the biomass fresh samplings were obtained, we imported in R in the xlsx file format that contained the georeferenced positions of samples by using the "read_excel" function of readxl R package (Wickham, 2016). Then the "extract" function of the raster R package (Hijmans et al., 2011) was used to extract the values corresponding to the crop sampling in a data-frame format. Then the data-frame object created was exported in a csv file format by using the "write.csv" function of the Utilis R package (R Core Team, 2018).

2.4 | Statistical analysis

All statistical analyses were performed with R statistical software (ver. 3.5.1., 2018). In order to select the model that could fit better with the data, several models were built and then the best model was selected based on the statistics that put a penalty on "complexity," such as the Akaike Information Criterion (Akaike, 1974) the Bayesian Information Criterion (Schwarz, 1978) and likelihood ratio tests (Wilks, 1938). The best model that fits better with the data is the mixed model, as reported by several studies (Onofri et al., 2016; Piepho et al., 2004). For data acquired during crop development (SPAD, dry biomass per meter square, and NDRE), the fixed factors of the mixed model were N and Zadoks scale and the random factors of the mixed model were year, block, plot, and zone management. While for the yield and soil data, the fixed factor of the mixed model was the N input, and the random factors of the mixed model were block, plot, and year.

Before performing the analysis of variance (ANOVA), it has been verified if the model meets the three assumptions of the ANOVA. The normality distribution of the model residual was checked both graphically (QQ plot) and by performing the Shapiro–Wilk normality test. Moreover, the homoscedasticity was checked using the Levene test. The last ANOVA assumption was satisfied by the experimental design and the random sampling. When all three ANOVA assumptions were met, the ANOVA was applied to the model. Only when the ANOVA showed a significant difference between the factors (p-value < 0.05), the estimated marginal means post hoc analysis was performed by using the "emmeans" function with the Bonferroni adjustment of the emmeans R package (Lenth, 2019).

2.4.1 | Zone management delineation

The zone management map creation workflow was entirely performed with R statistical software (ver. 3.5.1., 2018). The workflow to generate the management zone map is composed of several steps, which could be summarized as (1) stack layer generation, (2) subset stack layer only on the undistributed area, (3) cluster analysis, and (4) zone management map creation. To create a single stack layer on which to perform the analysis, the single NDRE raster layers must have the same spatial resolution. To obtain two raster layers with the same spatial resolution, the "resample" function of the raster R package (Hijmans et al., 2011) was used, which transfers values between nonmatching raster layers in terms of spatial resolution.

The unique stack layer contained NDRE raster layers created by using the "stack" function of the raster R package on the previously elaborated single raster layers. The cluster analysis was performed by using the "kmeans" function of the stats R package (3.5.1., 2018). To define the right value

TABLE 6 Results of analysis of variance (ANOVA) applied to the mixed model and the estimated marginal means analysis for the soil properties of both sites.

			C/N		Organic matter (g kg^{-1})		Nitrogen (g kg^{-1})	
Site	**Nitrogen input**	***df***	**Mean**	**Standard deviation**	**Mean**	**Standard deviation**	**Mean**	**Standard deviation**
LTE	N0		7.95a	0.66	13.53a	1.46	0.99a	0.02
	N90		7.8a	0.46	12.88a	0.35	0.96a	0.05
	N180		8.28a	0.57	15.18a	1.8	1.06a	0.07
Farm	N90		8.18a	0.44	13.7a	0.84	0.98a	0.03
	N222		7.76a	0.49	14.9a	1.68	1.11a	0.08
	Factors		*p*-Value		*p*-Value		*p*-Value	
LTE	N	2	n.s.		n.s.		n.s.	
Farm	N	1	n.s.		n.s.		n.s.	

Note: Means within column that are followed by the same letter are not significantly different at $p < 0.05\%$; n.s.: not significant at $p > 0.05$.
Abbreviations: C/N, carbon-nitrogen ratio; LTE, long-term experiment.

associated with the "centers" parameter of the "kmeans" function, the gap statistic index was performed, which calculates the goodness of clustering and defines the optimal number of clusters (Maechler et al., 2015).

The gap statistic compares the total intracluster variation for different values of k with their expected values under the null reference distribution of the data. Based on the gap statistic index, the k-means cluster analysis was performed, and the zone management map was created and then exported in an ESRI Shapefile file format with the "writeOGR" function of the rgdal R package (Bivand et al., 2013).

3 | RESULTS

3.1 | Soil properties

The ANOVA applied to the mixed model fitted with the soil properties data showed that the N input did not significantly affect the C/N, soil organic matter (g kg^{-1}), and soil N (g kg^{-1}) content in both sites (Table 6).

The estimated marginal means analysis did not raise any difference between the different N levels (Table 6). The LTE site showed a mean value of C/N higher than the farm site of +0.04, while for the other two soil properties, the farm site showed a higher mean value of +0.44 and +0.042 than the LTE site, respectively, for soil organic matter (g kg^{-1}) and soil N (g kg^{-1}).

3.2 | Soil Plant Analysis Development (SPAD) readings, dry biomass, and remote sensing

The ANOVA applied to the mixed model fitted with the SPAD readings, dry biomass (g m^{-2}), and NDRE showed that the N input and the ZS single effects can affect significantly all the variables in both sites (Table 7). Moreover, the combined effect of N input and ZS showed a significant difference in all the variables, and this led us to perform a statistical post hoc analysis on the combined effect to raise the differences between all the combinations (Table 7).

The estimated marginal means post hoc analysis showed that the higher the amount of nitrogen applied to the crop, the greater the response of each variable, site, and phenological stage (Table 7).

In more detail, the mean value of all variables obtained for N180 at the LTE site over the 3 years was statistically different from N0 and N90 treatments for each phenological stage and variable (Table 7). After the first N fertilization application at the end of tillering (ZS35), N180 over the 3 years had higher mean values of SPAD, dry biomass per square meter (g m^{-2}), and NDRE, respectively, of +7.9 (+15.2%), +194.7 (+49.8%), and +0.1 (+29.0%) than the N90 treatment. While after the second dose of fertilization, before head emergence (ZS60), N180 showed higher mean values of +6.5 (+12.0%), +448.8 (+36.0%), and +0.10 (+19.0%), respectively, for SPAD readings, dry biomass per square meter (g m^{-2}) and NDRE over the three years than N90 treatment (Table 7).

3.3 | Yield data

The ANOVA showed that the single effect of N input significantly impacts the grain yield (t ha^{-1}) in both sites (Table 8).

According to the estimated marginal means analysis results for the grain yield (t ha^{-1}), the higher the amount of N input applied to the crop, the greater the response of grain yield (t ha^{-1}) for both sites (Table 8). The grain yield (t ha^{-1})

TABLE 7 Results of analysis of variance (ANOVA) applied to the mixed model and the estimated marginal means analysis for SPAD, dry biomass, and normalized difference red edge index (NDRE) of both sites.

					SPAD		Dry biomass (g m^{-2})		NDRE	
Site	Year	ZS	Nitrogen input	*df*	Mean	Standard deviation	Mean	Standard deviation	Mean	Standard deviation
LTE	2018	35	N0		21.29c	2.8	101.59c	28.76	0.13c	0.01
			N90		42.32b	1.68	273.73b	23.09	0.26b	0.01
			N180		50.46a	0.61	405.04a	27.41	0.40a	0.03
		60	N0		15.11c	1.23	235.73c	63.83	0.15c	0.01
			N90		44.15b	0.82	538.45b	141.33	0.39b	0.02
			N180		52.12a	2.12	959.88a	191.77	0.47a	0.03
	2019	35	N0		33.75c	2.54	96.31c	36.99	0.20c	0.03
			N90		48.82b	1.88	211.00b	31.52	0.43b	0.02
			N180		55.87a	0.98	464.96a	58.19	0.55a	0.02
		60	N0		26.97c	5.69	381.89c	73.93	0.28c	0.05
			N90		50.86b	1.12	1064.33b	267.33	0.54b	0.01
			N180		56.93a	1.14	1482.64a	275.01	0.61a	0.01
	2020	35	N0		25.98c	3.5	18.51c	8.02	0.14c	0.01
			N90		41.45b	1.47	103.16b	31.12	0.24b	0.02
			N180		50.02a	0.96	302.08a	28.4	0.36a	0.02
		60	N0		30.54c	1.63	147.49c	72.07	0.22c	0.01
			N90		48.05b	2.82	793.27b	255.36	0.31b	0.02
			N180		53.48a	2.15	1299.8a	180.48	0.45a	0.02
Farm	2020	35	N90		37.68b	2.58	131.1b	37.53	0.32b	0.04
			N222		47.61a	1.45	398.27a	94.98	0.45a	0.05
		60	N90		41.10b	1.16	696.72b	166.41	0.36b	0.06
			N222		51.41a	0.72	1360.34a	264.05	0.53a	0.04

	Factors		*p*-Value	*p*-Value	*p*-Value
LTE	N[5]	2	***	***	***
	ZS	5	***	***	***
	N × ZS	10	***	***	***
Farm	N	1	***	*	**
	ZS	1	***	***	**
	N × ZS	1	***	*	***

Note: Within columns, numbers that are followed by the same letter are not significantly different at $p < 0.05$.

Abbreviations: LTE, long-term experiment; NDRE, normalized difference red edge index; SPAD, Soil Plant Analysis Development; ZS, Zadoks scale; ZS35, stem elongation; ZS60, anthesis.

*, **, and *** denote significance at $p < 0.05$, $p < 0.01$, and $p < 0.001$, respectively.

measured at the LTE site at the N180 showed higher values of +2.00 (+31.2%) and +5.17 (+80.5%) than N90 and N0. Instead, N90 showed a higher value (+71.7%) of grain yield (t ha^{-1}) than N0.

At the farm site during the 2019–2020 growing season, the N222 showed a statistically higher value of +1.6 (+24.6%) grain yield (t ha^{-1}) than N90. The N222 treatment at the farm site yielded 1.8% higher than treatment N180 at the LTE site, and therefore the 42 units of higher N does not justify an increase in yield. While considering the N90 treatment of the farm site and LTE, no notable differences are shown (Table 8).

3.4 | Zone management map—Long-term experimental site

The six NDRE vegetation index maps of the LTE were set to the same scale as the farm site, which helps in better

TABLE 8 Results of analysis of variance (ANOVA) applied to the mixed model and the estimated marginal means analysis for the grain yield (t ha^{-1}) of both sites.

				Grain yield (t ha^{-1})	
Site	**Year**	**Nitrogen input**	***df***	**Mean**	**Standard deviation**
LTE[2]	2020	N0		1.25c	0.26
		N90		4.42b	0.22
		N180		6.42a	0.22
Farm	2020	N90		4.93b	0.57
		N222		6.54a	0.92
	Factors			*p*-Value	
LTE	N		2	**	
Farm	N		1	*	

Note: Means within column that are followed by the same letter are not significantly different at $p < 0.05$.
Abbreviations: LTE, long-term experiment.
* and ** denote significance $p < 0.05$ and $p < 0.01$, respectively. n.s., not significant at $p > 0.05$.

understanding the changes resulting due to different years, phenological stages, and sites.

Moving from one phenological stage to the next (ZS35 and ZS60), the NDRE maps (Figure 4) show an increase in values as reported in Table 7 and also allow us to strongly emphasize the differences related to the experimental design and the different levels of fertilization applied to the crop.

The gap statistic index was applied in the stack layer object and showed that the optimal number of clusters of the "kmeans" function in the LTE site for both years under analysis was 3 (Figure 5), and the results of this unsupervised machine learning algorithm are shown in Figure 5.

The three resulting clusters fitted well with the LTE experimental design, where the N0 was related to the first cluster, the N90 was related to the second cluster, and the N180 was related to the third cluster.

3.5 | Zone management map—Farm site

Starting from the phenological stage ZS35 until reaching the ZS60 phenological stage (Figure 6), the NDRE maps showed an increase in values as reported in Table 7. Moreover, the NDRE maps (Figure 6) emphasize the differences between the two areas at different doses of N fertilization applied to the crop.

The gap statistic index showed that the optimal number of clusters of the "kmeans" function in the farm site was 2 (Figure 7), and the results of this unsupervised machine learning algorithm are shown in Figure 7.

The two resulting clusters fitted well with the farm experimental site where the N90 was related to the first cluster and the N222 was related to the second cluster.

4 | DISCUSSION

4.1 | Soil properties

The chemical soil properties such as C/N, soil organic matter (g kg^{-1}), and soil N availability (g kg^{-1}) were not affected by different levels of N fertilization, this is due to the well-known N high mobility in the soil (Bhattacharyya et al., 2017; Zhong et al., 2014).

Several authors reported that when a longer time frame is considered, different N rates can significantly affect many chemical soil properties such as soil acidification, salinity, oxidation reactions, and exchange capacity (Ata-Ul-Karim et al., 2020). When these chemical soil properties change, it indirectly affects the soil microbial composition, which are the bio-producers of organic matter, and so the soil nitrogen availability (Deligios et al., 2017).

Moreover, Ata-Ul-Karim et al. (2020) and Bhattacharyya et al. (2017) reported several studies where excessive N fertilization may impair soil health through negative effects on the soil biological community, which are the bio-producers of the N form that the crops then absorb to complete the biological cycle.

4.2 | Remote-proximal sensing and crop variables

The higher the N input is applied to the crop, the greater the biomass produced by the crop for each year, site, and phenological stage under analysis (Pro et al., 2021). This pattern of crop development was also detected by remote and proximal sensing tools (Fiorentini et al., 2021). These tools can be used to continuously monitor the spatial-temporal variability

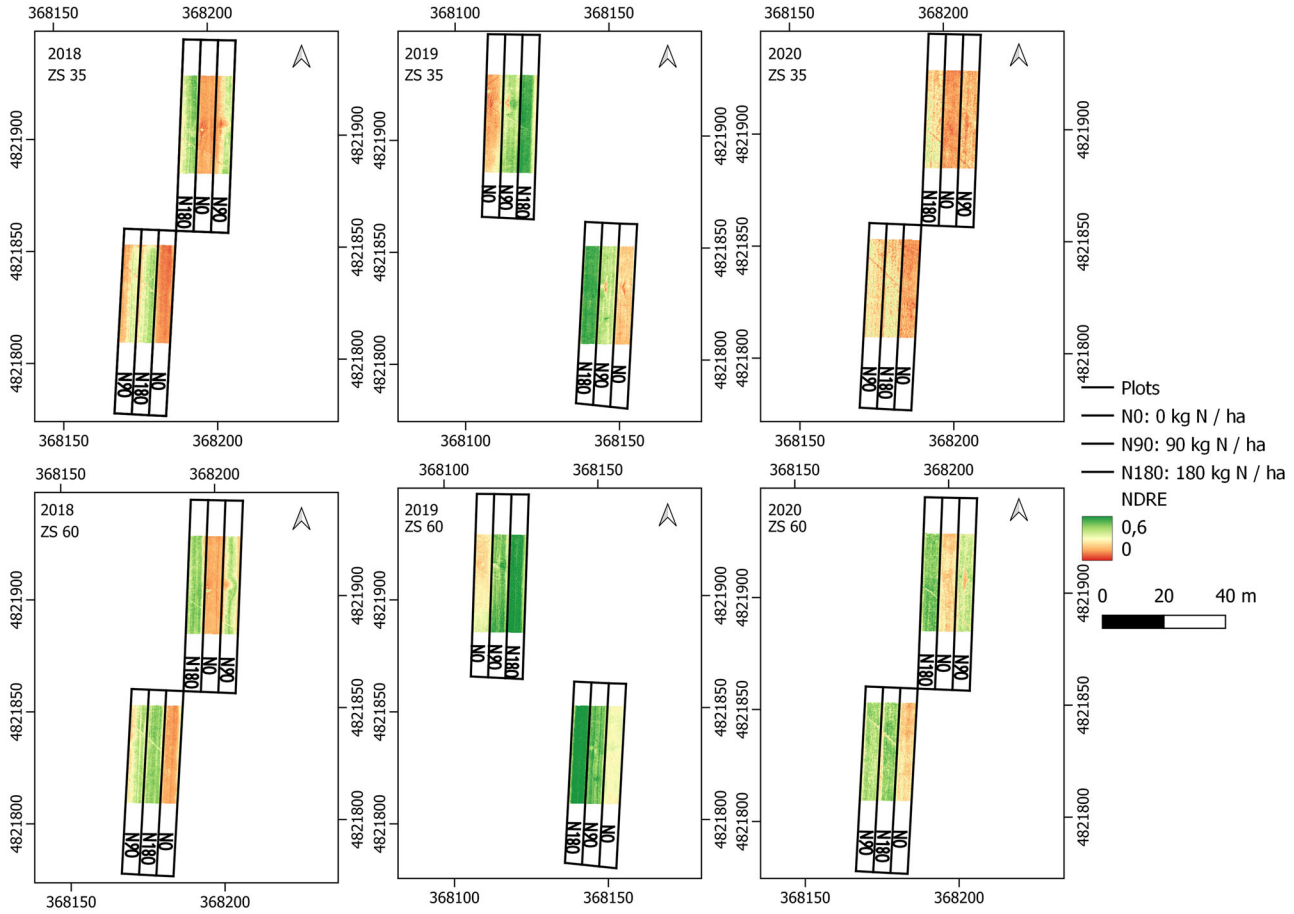


FIGURE 4 Experimental design and normalized difference red edge index (NDRE) vegetation index at stem elongation (ZS35) and at anthesis (ZS60) of the three growing seasons at the long-term experiment (LTE) site.

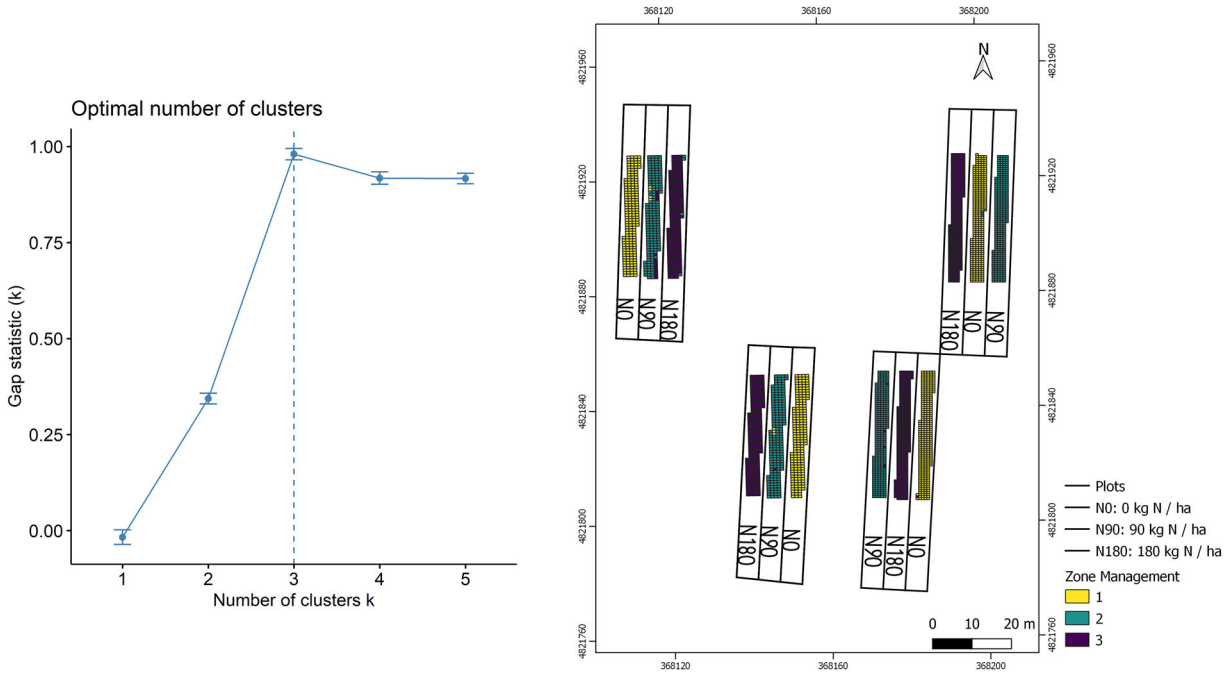


FIGURE 5 The optimal number of clusters based on the gap statistic index for both growing seasons (2018, 2019, and 2020) and the zone management of the long-term experiment (LTE).

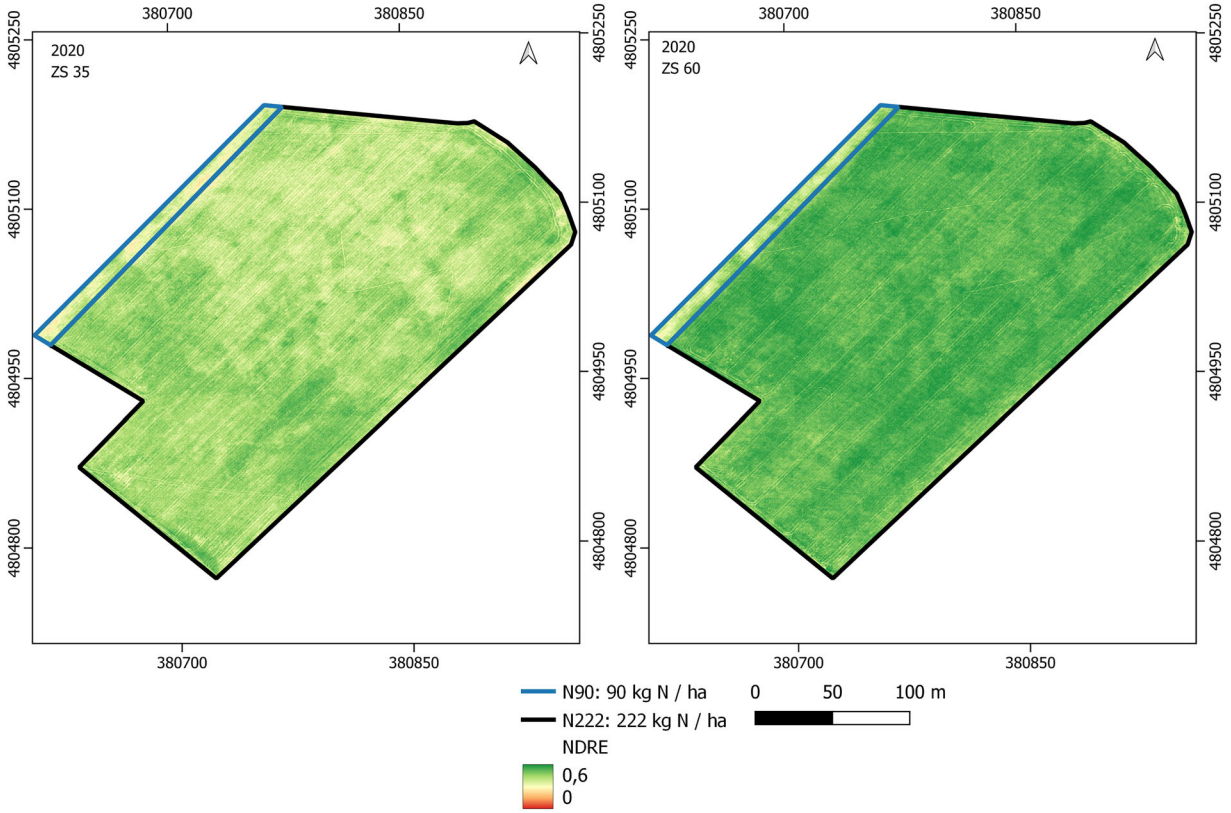


FIGURE 6 Normalized difference red edge index (NDRE) vegetation index at stem elongation (ZS35) of 2020 growing season of the farm site. ZS60, anthesis.

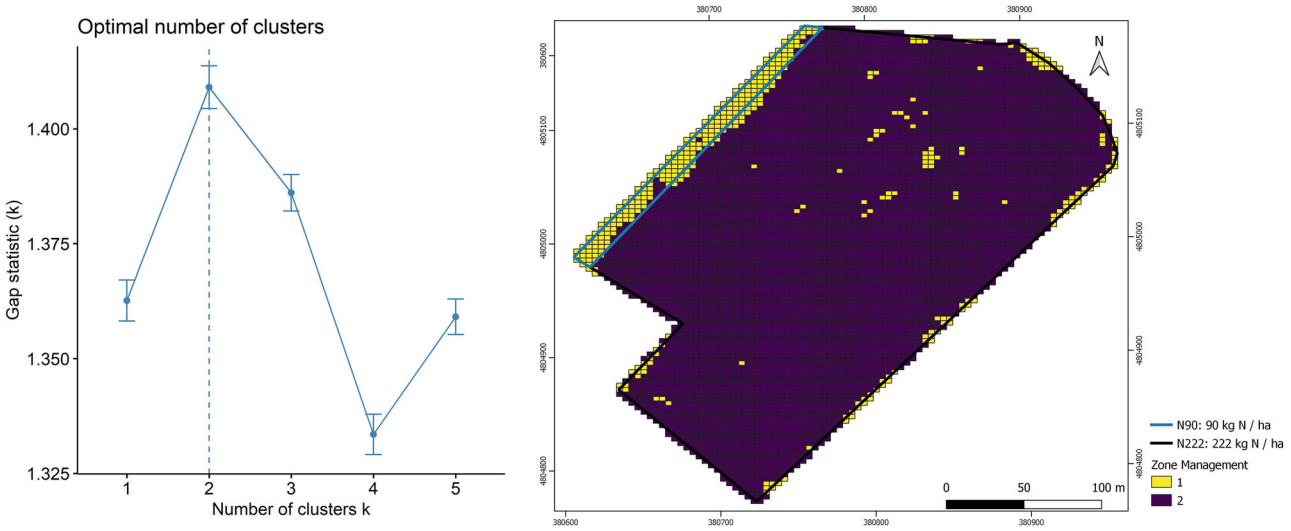


FIGURE 7 The optimal number of clusters based on the gap statistic index of the 2020 growing season and the zone management of the farm site.

during the entire growing season, which is fundamental to the SSM applications.

A review performed by Mulla (2013) reported that remote sensing technologies can effectively follow the leaf area index, biomass, crop density, yield potential estimation, and detection and mapping of biotic and abiotic stresses.

In Spain, seven different inorganic N rates were applied in maize, and Maresma et al. (2016) showed that the higher the

N input applied to the crop, the greater the NDVI, WDRVI, GRVI, and SPAD values. Also, Argento et al. (2020) in four different sites in Switzerland showed that the vegetation index is well related to crop variables such as dry matter, N uptake, and nitrogen nutrition index. Moreover, Argento et al. (2020) showed that NDRE was the best vegetation index to be related to the crop variables as reported by Fiorentini et al. (2019). Moreover, Schillaci et al. (2020) reported that the vegetation indexes could offer a picture of the nutritional status of the crop and could be integrated into a spatial-temporal decision support system to optimize the maize N fertilization at the farm scale.

But it is also equally true that each vegetation index has its specific expression of green vegetation, its suitability for specific uses, and some limiting factors. Therefore, for practical applications, the choice of a specific vegetation index needs to be made with caution by comprehensively considering and analyzing the advantages and limitations of existing vegetation indexes and then combining them to be applied in a specific environment. In this way, the use of vegetation indexes can be tailored to specific applications, instrumentation used, and platforms (Xue & Su, 2017). Therefore, it is essential that the scientific–agronomic community test and validate which vegetation index is most appropriate to use based on the soil and climate conditions, crops, and cultivars used in the area.

4.3 | Management zones and yield data

The environmental and economic benefits of PA pass through the most famous applications such as the SSM (Albarenque et al., 2016; Pantazi et al., 2020). Therefore, the determination of the number and location of homogeneous zones is fundamental, and nowadays many approaches and operational software define the number of zones in an arbitrary and constant way, such as high-, medium-, and low-input zones, without a priori statistical analysis and validation. These methods must be validated using statistical analyses of yield data before being implemented on an operational scale (Gavioli et al., 2019; Nawar et al., 2017).

Several authors study the best approaches that can determine such areas (Janrao & Palivela, 2015; Yuan et al., 2022) but such approaches should be designed to be used at an operational scale. For a method to be considered operational, it must be automatic, must have as its data source that is free and temporally-spatially accurate (e.g., multispectral satellite data), must be used in any field, and scientifically validated.

Gavioli et al. (2019) evaluated 20 different algorithms for defining and validating zone management in commercial fields of soybean and maize in Brazil with yield data. The number of clusters analyzed were two, three, and four, and after the comprehensive analysis, the number of zones was set for each field. While Denora, Fiorentini, et al. (2022) and Yuan et al. (2022) used source data as input of the workflow to generate the zone management of the soil data that can be measured with hand-acquired data or with the aid of electromagnetic sensors. All the previous works use proximal sensing data as source data, and the procedures for determining the number and location of zones were not performed automatically so it is difficult to scale.

Our contribution to this theme was to test an automatic approach to delineate the homogeneous zones starting from multispectral images in two different sites and then agronomically validate this approach with the typical agronomic crop sampling activity and statistical analysis. The approach was able to fit with the experimental design of both sites, and statistical analysis showed differences in yields between the zone management due to the different N levels for both sites (Karpinski et al., 2015). This approach could be scaled at a large scale by using the freely accessible multispectral images obtainable by Sentinel 2 Copernicus constellation.

5 | CONCLUSIONS

Although N fertilization has several negative environmental and social impacts, it also improves crop yield, farmer income, and global food security. An opportunity exists to further enhance the yield, and profitability, and reduce the environmental impacts of agricultural activity through the SSM, which is the most common and operational activity of the PA applications. To implement the SSM, it is necessary to perform a continuous monitoring activity of the crop status during the entire growing season with spatial-temporal data and define the number and location of homogeneous zones. Nowadays, many approaches are used to define the number of zones in an arbitrary and constant way, such as high-, medium-, and low-input zones, without a priori statistical analysis, and it is difficult to use them as source data at the operational level.

The approach here reported showed the potential of multispectral images to be used as input data of an automatic workflow to delineate the management zones to apply the SSM. The management zones delineated by the automatic approach were agronomically validated by on-season crop sampling and multi-site/year yield data. The workflow could be scaled to bigger areas by using as source free multispectral data of the "Sentinel-2" Copernicus Satellites constellation.

AUTHOR CONTRIBUTIONS

Roberto Orsini: Conceptualization; funding acquisition; methodology; project administration; supervision; writing—original draft. **Marco Fiorentini**: Data curation; formal analysis; methodology; software; validation; writing—review and editing. **Stefano Zenobi**: Data curation; investigation; methodology; validation. **Rodolfo Santilocchi**:

Conceptualization; supervision. **Paola A. Deligios**: Investigation; supervision; writing—review and editing. **Luigi Ledda**: Conceptualization; investigation; supervision.

ACKNOWLEDGMENTS

This work is supported by Marche Polytechnic University, through University Strategic Project (PSA 2017) "PFRLab: Setting of a Precision Farming Robotic Laboratory for Cropping System Sustainability and Food Safety and Security", Marche Region through measure 16.1 Action 2 of the Rural Development Plan (PSR 2014/2020) "Precision agriculture: reduction of the environmental impact of production systems" (project ID 29000), and HORIZON 2020 Project (H2020) number 952879, SolAcqua.

CONFLICT OF INTEREST STATEMENT

The authors declare no conflicts of interest.

ORCID

Marco Fiorentini https://orcid.org/0000-0002-1101-7313
Paola A. Deligios https://orcid.org/0000-0001-9724-2812

REFERENCES

Akaike, H. (1974). A new look at the statistical model identification. *IEEE Transactions on Automatic Control*, *19*, 716–723. https://doi.org/10.1109/TAC.1974.1100705

Albarenque, S. M., Basso, B., Caviglia, O. P., & Melchiori, R. J. M. (2016). Spatio-temporal nitrogen fertilizer response in maize: Field study and modeling approach. *Agronomy Journal*, *108*, 2110–2122. https://doi.org/10.2134/agronj2016.02.0081

Ali, A., Rondelli, V., Martelli, R., Falsone, G., Lupia, F., & Barbanti, L. (2022). Management zones delineation through clustering techniques based on soils traits, NDVI data, and multiple year crop yields. *Agriculture*, *12*, 231. https://doi.org/10.3390/agriculture12020231

Aqeel-Ur-Rehman, Abbasi, A. Z., Islam, N., & Shaikh, Z. A. (2014). A review of wireless sensors and networks' applications in agriculture. *Computer Standards & Interfaces*, *36*, 263–270. https://doi.org/10.1016/j.csi.2011.03.004

Argento, F., Anken, T., Abt, F., Vogelsanger, E., Walter, A., & Liebisch, F. (2020). Site-specific nitrogen management in winter wheat supported by low-altitude remote sensing and soil data. *Precision Agriculture*, *22*, 364–386. https://doi.org/10.1007/s11119-020-09733-3

Ata-Ul-Karim, S. T., Cang, L., Wang, Y., & Zhou, D. (2020). Interactions between nitrogen application and soil properties and their impacts on the transfer of cadmium from soil to wheat (*Triticum aestivum* L.) grain. *Geoderma*, *357*, 113923. https://doi.org/10.1016/j.geoderma.2019.113923

Barnes, E. M., Clarke, T. R., Richards, S. E., Colaizzi, P. D., Haberland, J., Kostrzewski, M., Waller, P., Choi, C., Riley, E., & Thompson, T. (2000). Coincident detection of crop water stress, nitrogen status and canopy density using ground based multispectral data. In *Proceedings of the fifth International Conference on Precision Agriculture*. ISPAG.

Bhattacharyya, R., Kundu, S., Thind, H. S., Ghosh, B. N., Sarkar, D., Batabyal, K., Mandal, B., Rajendiran, S., Anil, K. S., & Lalitha, M. (2017). Nitrogen and soil quality. In Y. P. Abrol, T. K. Adhya, V. P. Aneja, N. Raghuram, H. Pathak, U. Kulshrestha, C. Sharma, & B. Singh (Eds.), *The Indian nitrogen assessment: Sources of reactive nitrogen, environmental and climate effects, management options, and policies* (pp. 219–233). Elsevier. https://doi.org/10.1016/B978-0-12-811836-8.00015-X

Bivand, R., Keitt, T., & Rowlingson, B. (2013). *rgdal: Bindings for the geospacial data abstraction library*. https://cran.r-project.org/web/packages/rgdal/index.html

Capmourteres, V., Adams, J., Berg, A., Fraser, E., Swanton, C., & Anand, M. (2018). Precision conservation meets precision agriculture: A case study from southern Ontario. *Agricultural Systems*, *167*, 176–185. https://doi.org/10.1016/j.agsy.2018.09.011

Castrignanò, A., Buttafuoco, G., Quarto, R., Parisi, D., Viscarra Rossel, R. A., Terribile, F., Langella, G., & Venezia, A. (2018). A geostatistical sensor data fusion approach for delineating homogeneous management zones in precision agriculture. *Catena*, *167*, 293–304. https://doi.org/10.1016/j.catena.2018.05.011

Chai, R., Ye, X., Ma, C., Wang, Q., Tu, R., Zhang, L., & Gao, H. (2019). Greenhouse gas emissions from synthetic nitrogen manufacture and fertilization for main upland crops in China. *Carbon Balance and Management*, *14*, Article 20. https://doi.org/10.1186/s13021-019-0133-9

Chlingaryan, A., Sukkarieh, S., & Whelan, B. (2018). Machine learning approaches for crop yield prediction and nitrogen status estimation in precision agriculture: A review. *Computers and Electronics in Agriculture*, *151*, 61–69. https://doi.org/10.1016/j.compag.2018.05.012

Dawson, C. J., & Hilton, J. (2011). Fertiliser availability in a resource-limited world: Production and recycling of nitrogen and phosphorus. *Food Policy*, *36*, S14–S22. https://doi.org/10.1016/j.foodpol.2010.11.012

Deligios, P. A., Chergia, A. P., Sanna, G., Solinas, S., Todde, G., Narvarte, L., & Ledda, L. (2019). Climate change adaptation and water saving by innovative irrigation management applied on open field globe artichoke. *Science of the Total Environment*, *649*, 461–472. https://doi.org/10.1016/j.scitotenv.2018.08.349

Deligios, P. A., Tiloca, M. T., Sulas, L., Buffa, M., Caraffini, S., Doro, L., Sanna, G., Spanu, E., Spissu, E., Urracci, G. R., & Ledda, L. (2017). Stable nutrient flows in sustainable and alternative cropping systems of globe artichoke. *Agronomy for Sustainable Development*, *37*, Article 54. https://doi.org/10.1007/s13593-017-0465-3

Denora, M., Amato, M., Brunetti, G., De Mastro, F., & Perniola, M. (2022). Geophysical field zoning for nitrogen fertilization in durum wheat (*Triticum durum* Desf.). *PLoS One*, *17*, e0267219. https://doi.org/10.1371/journal.pone.0267219

Denora, M., Fiorentini, M., Zenobi, S., Deligios, P. A., Orsini, R., Ledda, L., & Perniola, M. (2022). Validation of rapid and low-cost approach for the delineation of zone management based on machine learning algorithms. *Agronomy*, *12*, 183. https://doi.org/10.3390/agronomy12010183

Fiorentini, M., Schillaci, C., Denora, M., Zenobi, S., Deligios, P., Orsini, R., Santilocchi, R., Perniola, M., Montanarella, L., & Ledda, L. (2022). A machine learning modelling framework for *Triticum turgidum* subsp. *durum* Desf. yield forecasting in Italy. *Agronomy Journal*. https://doi.org/10.1002/agj2.21279

Fiorentini, M., Zenobi, S., Giorgini, E., Basili, D., Conti, C., Pro, C., Monaci, E., & Orsini, R. (2019). Nitrogen and chlorophyll status determination in durum wheat as influenced by fertilization and soil management: Preliminary results. *PLoS One*, *14*, e0225126. https://doi.org/10.1371/journal.pone.0225126

Fiorentini, M., Zenobi, S., & Orsini, R. (2021). Remote and proximal sensing applications for durum wheat nutritional status detection in Mediterranean area. *Agriculture*, *11*, 39. https://doi.org/10.3390/AGRICULTURE11010039

Gavioli, A., De Souza, E. G., Bazzi, C. L., Schenatto, K., & Betzek, N. M. (2019). Identification of management zones in precision agriculture: An evaluation of alternative cluster analysis methods. *Biosystems Engineering*, *181*, 86–102. https://doi.org/10.1016/j.biosystemseng.2019.02.019

Hijmans, R. J., van Etten, J., Mattiuzzi, M., Sumner, M., Greenberg, J. A., Lamigueiro, O. P., Bevan, A., Racine, E. B., & Shortridge, A. (2011). *Raster*. https://cran.r-project.org/web/packages/raster/index.html

Janrao, P., & Palivela, H. (2015). Management zone delineation in Precision agriculture using data mining: A review. In *2015 International Conference on Innovations in Information, Embedded and Communication Systems* (ICIIECS) (pp. 1–7). IEEE. https://doi.org/10.1109/ICIIECS.2015.7193256

Karpinski, I., Schuler, J., & Müller, K. (2015). A new approach to support site-specific farming and economic decision making for precision agriculture in East Germany: The heterogeneity indicator. *Outlook on Agriculture*, *44*, 283–289. https://doi.org/10.5367/oa.2015.0224

Langholtz, M., Davison, B. H., Jager, H. I., Eaton, L., Baskaran, L. M., Davis, M., & Brandt, C. C. (2021). Increased nitrogen use efficiency in crop production can provide economic and environmental benefits. *Science of the Total Environment*, *758*, 143602. https://doi.org/10.1016/j.scitotenv.2020.143602

Lenth, R. (2019). *Emmeans: Estimated marginal means, aka least-squares means*. https://cran.r-project.org/web/packages/emmeans/index.html

Maechler, M., Struyf, A., Hubert, M., Hornik, K., Studer, M., & Roudier, P. (2015). *Package 'cluster': Cluster analysis basics and extensions*. https://cran.r-project.org/web/packages/cluster/index.html

Maes, W. H., & Steppe, K. (2019). Perspectives for remote sensing with unmanned aerial vehicles in precision agriculture. *Trends in Plant Science*, *24*, 152–164. https://doi.org/10.1016/j.tplants.2018.11.007

Maresma, Á., Ariza, M., Martínez, E., Lloveras, J., & Martínez-Casasnovas, J. (2016). Analysis of vegetation indices to determine nitrogen application and yield prediction in maize (*Zea mays* L.) from a standard UAV service. *Remote Sensing*, *8*, 973. https://doi.org/10.3390/rs8120973

Migliorini, P., Moschini, V., Tittarelli, F., Ciaccia, C., Benedettelli, S., Vazzana, C., & Canali, S. (2014). Agronomic performance, carbon storage and nitrogen utilisation of long-term organic and conventional stockless arable systems in Mediterranean area. *European Journal of Agronomy*, *52*, 138–145. https://doi.org/10.1016/j.eja.2013.09.017

Mulla, D. J. (2013). Twenty five years of remote sensing in precision agriculture: Key advances and remaining knowledge gaps. *Biosystems Engineering*, *114*, 358–371. https://doi.org/10.1016/j.biosystemseng.2012.08.009

Munnaf, M. A., Haesaert, G., & Mouazen, A. M. (2021). Map-based site-specific seeding of seed potato production by fusion of proximal and remote sensing data. *Soil and Tillage Research*, *206*, 104801. https://doi.org/10.1016/j.still.2020.104801

Nawar, S., Corstanje, R., Halcro, G., Mulla, D., & Mouazen, A. M. (2017). Delineation of soil management zones for variable-rate fertilization: A review. In D. L. Sparks (Ed.), *Advances in agronomy* (pp. 175–245). Academic Press. https://doi.org/10.1016/bs.agron.2017.01.003

Onofri, A., Seddaiu, G., & Piepho, H.-P. (2016). Long-term experiments with cropping systems: Case studies on data analysis. *European Journal of Agronomy*, *77*, 223–235. https://doi.org/10.1016/j.eja.2016.02.005

Orsini, R., Basili, D., Belletti, M., Bentivoglio, D., Bozzi, C. A., Chiappini, S., Conti, C., Galli, A., Giorgini, E., Fiorentini, M., Malinverni, E. S., Mancini, A., Mazzanti, L., Monaci, E., Passerini, G., Pro, C., Santilocchi, R., Vignini, A., Zenobi, S., & Zingaretti, P. (2019a). Setting of a precision farming robotic laboratory for cropping system sustainability and food safety and security: Preliminary results. *IOP Conference Series: Earth and Environmental Science*, *175*, 012021. https://doi.org/10.1088/1755-1315/275/1/012021

Orsini, R., Fiorentini, M., & Zenobi, S. (2019b). Testing vegetation index categories as influenced by soil management and nitrogen fertilization in cereal based cropping systems. In *2019 IEEE international workshop on metrology for agriculture and forestry (MetroAgriFor)* (pp. 13–18). IEEE. https://doi.org/10.1109/MetroAgriFor.2019.8909216

Pantazi, X. E., Moshou, D., & Bochtis, D. (2020). Utilization of multisensors and data fusion in precision agriculture. *Intelligent data mining and fusion systems in agriculture* (pp. 103–173). Elsevier. https://doi.org/10.1016/b978-0-12-814391-9.00003-0

Peng, J., Xu, Y., Shang, B., Qu, L., & Feng, Z. (2020). Impact of ozone pollution on nitrogen fertilization management during maize (*Zea mays* L.) production. *Environmental Pollution*, *266*, 115158. https://doi.org/10.1016/j.envpol.2020.115158

Piepho, H. P., Buchse, A., & Richter, C. (2004). A mixed modelling approach for randomized experiments with repeated measures. *Journal of Agronomy and Crop Science*, *190*, 230–247. https://doi.org/10.1111/j.1439-037X.2004.00097.x

Pro, C., Basili, D., Notarstefano, V., Belloni, A., Fiorentini, M., Zenobi, S., Alia, S., Vignini, A., Orsini, R., & Giorgini, E. (2021). A spectroscopic approach to evaluate the effects of different soil tillage methods and nitrogen fertilization levels on the biochemical composition of durum wheat (*Triticum turgidum* subsp. *durum*) leaves and caryopses. *Agriculture*, *11*, 321. https://doi.org/10.3390/agriculture11040321

Puertes, C., Bautista, I., Lidón, A., & Francés, F. (2021). Best management practices scenario analysis to reduce agricultural nitrogen loads and sediment yield to the semiarid Mar Menor coastal lagoon (Spain). *Agricultural Systems*, *188*, 103029. https://doi.org/10.1016/j.agsy.2020.103029

R Core Team. (2018). *A language and environment for statistical computing*. R Foundation for Statistical Computing. https://www.r-project.org/

Rath, S., Zamora-Re, M., Graham, W., Dukes, M., & Kaplan, D. (2021). Quantifying nitrate leaching to groundwater from a corn-peanut rotation under a variety of irrigation and nutrient management practices in the Suwannee River Basin, Florida. *Agricultural Water Management*, *246*, 106634. https://doi.org/10.1016/j.agwat.2020.106634

Schillaci, C., Perego, A., Valkama, E., Märker, M., Saia, S., Veronesi, F., Lipani, A., Lombardo, L., Tadiello, T., Gamper, H. A., Tedone, L., Moss, C., Pareja-Serrano, E., Amato, G., Kühl, K., Dămătîrcă, C., Cogato, A., Mzid, N., Eeswaran, R., … Acutis, M. (2021). New pedotransfer approaches to predict soil bulk density using WoSIS soil data and environmental covariates in Mediterranean agro-ecosystems. *Science of the Total Environment*, *780*, 146609. https://doi.org/10.1016/j.scitotenv.2021.146609

Schillaci, C., Tomasoni, E., Acutis, M., & Perego, A. (2020). *Data assimilation of remote sensing data for farm scale maize fertilization in northern Italy* [EGU general assembly conference abstracts]. DISAA,

Agricultural and Environmental Sciences Production, Landscape, Agroenergy Department, University of Milan.

Schwarz, G. (1978). Estimating the dimension of a model. *The Annals of Statistics*, *6*, 461–464. https://doi.org/10.1214/aos/1176344136

Seddaiu, G., Iocola, I., Farina, R., Orsini, R., Iezzi, G., & Roggero, P. P. (2016). Long term effects of tillage practices and N fertilization in rainfed Mediterranean cropping systems: Durum wheat, sunflower and maize grain yield. *European Journal of Agronomy*, *77*, 166–178. https://doi.org/10.1016/j.eja.2016.02.008

Stettmer, M., Mittermayer, M., Maidl, F.-X., Schwarzensteiner, J., Hülsbergen, K.-J., & Bernhardt, H. (2022). Three methods of site-specific yield mapping as a data source for the delineation of management zones in winter wheat. *Agriculture*, *12*, 1128. https://doi.org/10.3390/agriculture12081128

Tsialtas, J. T., Theologidou, G. S., & Karaoglanidis, G. S. (2018). Effects of pyraclostrobin on leaf diseases, leaf physiology, yield and quality of durum wheat under Mediterranean conditions. *Crop Protection*, *113*, 48–55. https://doi.org/10.1016/j.cropro.2018.07.008

Vallentin, C., Dobers, E. S., Itzerott, S., Kleinschmit, B., & Spengler, D. (2020). Delineation of management zones with spatial data fusion and belief theory. *Precision Agriculture*, *21*, 802–830. https://doi.org/10.1007/s11119-019-09696-0

Verhoeven, G. (2011). Taking computer vision aloft–archaeological three-dimensional reconstructions from aerial photographs with photoscan. *Archaeological Prospection*, *18*, 67–73. https://doi.org/10.1002/arp.399

Wesseler, J. (2022). The EU's farm-to-fork strategy: An assessment from the perspective of agricultural economics. *Applied Economic Perspectives and Policy*, *44*, 1826–1843. https://doi.org/10.1002/aepp.13239

Whelan, B., & Mcbratney, A. (2003). Definition and interpretation of potential management zones in Australia. In *Proceedings of the 6th International Conference on Precision Agriculture and Other Precision Resources Management*. University of Minnesota, ISPAG.

Wickham, H. (2016). *readxl: Read Excel files*. https://cran.r-project.org/web/packages/readxl/index.html

Wilks, S. S. (1938). The large-sample distribution of the likelihood ratio for testing composite hypotheses. *The Annals of Mathematical Statistics*, *9*, 60–62. https://doi.org/10.1214/aoms/1177732360

Xue, J., & Su, B. (2017). Significant remote sensing vegetation indices: A review of developments and applications. *Journal of Sensors*, *2017*, Article 1353691. https://doi.org/10.1155/2017/1353691

Yuan, Y., Shi, B., Yost, R., Liu, X., Tian, Y., Zhu, Y., Cao, W., & Cao, Q. (2022). Optimization of management zone delineation for precision crop management in an intensive farming system. *Plants*, *11*, 2611. https://doi.org/10.3390/plants11192611

Zadoks, J. C., Chang, T. T., & Konzak, C. F. (1974). A decimal code for the growth stages of cereals. *Weed Research*, *14*, 415–421. https://doi.org/10.1111/j.1365-3180.1974.tb01084.x

Zhang, X., Shi, L., Jia, X., Seielstad, G., & Helgason, C. (2010). Zone mapping application for precision-farming: A decision support tool for variable rate application. *Precision Agriculture*, *11*, 103–114. https://doi.org/10.1007/s11119-009-9130-4

Zhong, H., Wang, Q., Zhao, X., Du, Q., Zhao, Y., Wang, X., Jiang, C., Zhao, S., Cao, M., Yu, H., & Wang, D. (2014). Effects of different nitrogen applications on soil physical, chemical properties and yield in maize (*Zea mays* L.). *Agricultural Sciences*, *5*, 1440–1447. https://doi.org/10.4236/as.2014.514155

How to cite this article: Orsini, R., Fiorentini, M., Zenobi, S., Santilocchi, R., Deligios, P. A., & Ledda, L. (2023). Automatic zone management definition in Mediterranean environment for *Triticum durum*. *Agrosystems, Geosciences & Environment*, *6,* e20422. https://doi.org/10.1002/agg2.20422